Natural Resources Canada | Ressources naturelles Canada

GEOLOGICAL SURVEY OF CANADA
OPEN FILE 8539

Failure mechanism of an ancient landslide at Low, Quebec

B. Wang

2019

Canada

GEOLOGICAL SURVEY OF CANADA
OPEN FILE 8539

Failure mechanism of an ancient landslide at Low, Quebec

B. Wang

2019

Permanent link: https://doi.org/10.4095/313557

This publication is available for free download through GEOSCAN (http://geoscan.nrcan.gc.ca/).

Recommended citation
Wang, B., 2019. Failure mechanism of an ancient landslide at Low, Quebec; Geological Survey of Canada, Open File 8539, 19 p. https://doi.org/10.4095/313557

Publications in this series have not been edited; they are released as submitted by the author.

Failure mechanism of an ancient landslide at Low, Quebec

Baolin Wang

ABSTRACT

This Open File presents a geotechnical study of a Champlain Sea clay landslide near the municipality of Low, Quebec. The landslide is one of 12 landslides identified from previous studies to have been triggered by an earthquake about 1020 cal yr BP. Geotechnical studies were conducted to investigate the failure mechanism of the landslide. This is one of three landslides investigated for the purpose of estimating the minimum magnitude of the earthquake. Field tests were conducted in and around the landslide zone. Micro-seismic surveys at 27 locations indicate the sediment thickness ranging from 10 m to 44 m below the current surface. Cone Penetrometer Tests (CPT) at four locations confirmed the micro-seismic measurements to be fairly accurate. The CPT tip resistance data were calibrated with field Vane Shear Test (VST) results. The soil peak undrained shear strength (C_u) is found to correlate with depth (H) from the original Champlain Sea surface as $C_u = 28 + 1.42H$. The test results and other information indicate that the 1020 cal yr BP landslide likely occurred inside a larger landslide zone of a much older age. The landslide is likely a flake type failure based on the data collected and by comparison with other cases. A slope model is constructed for stability analysis to determine the threshold ground acceleration required to trigger the failure. The resulting minimum horizontal ground acceleration is 0.19 g.

1. INTRODUCTION

An earthquake was hypothesized by Brooks (2013) to have occurred in the general Ottawa-Gatineau region of eastern Ontario-western Quebec about 1020 cal yr BP. The hypothesis is based on 10 landslides of common ages identified in the region. He calculated the earthquake magnitude to be a minimum 6.1 based on Keefer (1984) and Rodriguez et al. (1999) correlations. Brooks (2014a, 2014b, and 2015) later discovered two more landslides of similar ages along the Gatineau River valley further north of those other landslides previously identified. The data provide new evidence that further support the earthquake hypothesis. The finding of the earthquake is important for understanding the region's paleoseismicity. However, the correlations used for estimating the magnitude of the earthquake have limitations. All the 12 landslides identified above occurred in Champlain Sea clays. A main concern with the magnitude estimate is that the correlations used do not address the shaking amplification effect of soft clays. Another issue is that the slope failure mechanism of sensitive clays is significantly different from those of other landslides used for the correlations. A geotechnical study was therefore initiated to further investigate the magnitude of the earthquake from geotechnical signatures preserved with the landslides. Three of the 1020 cal yr BP landslides were selected for the paleoseismicity study. The approach is to reconstruct the slope and calculate the minimum ground acceleration required to trigger the failure at each site. The results are then used to triangulate the minimum magnitude of the earthquake. The three landslides selected are located at Quyon, Breckenridge and Low (all in Quebec) about 30 km to 38 km apart. Details of the Quyon and Breckenridge landslide studies have been reported in Wang (2016) and Wang (2018) respectively. This Open File presents the results from the Low site.

2. SITE DESCRIPTION

The study site is located at Stag Creek near Low, Quebec or about 50 km north-northwest from Ottawa, Ontario (Fig. 1). Stag Creek is a tributary to the Gatineau River. Regionally the topography is hilly with elevations ranging from about 100 m to 250 m above sea level (asl.). More locally, ground elevations vary from about 113 m at Stag Creek to about 170 m at nearby rock outcrops. Champlain Sea sediments are present in the relatively flat areas where the elevation is around 153 m. Access to the head scarp is via McCrank and O'Connor Roads (Fig. 1).

The elongated failure zone shown in Fig. 1 is about 790 m long and 430 m wide. It was originally inferred by Brooks (unpublished and personal communication) as one failure occurred about 1020 cal yr BP. However, data obtained from the current investigation as discussed later indicate that the scar zone is likely the result of two separate failures. The depth of the overall landslide depression is about 10 to 15 m below the original Champlain Sea plain. There are two distinct debris plateaus inside the scar zone as shown in Fig. 1. The elevation of the lower plateau is about 5 m below the upper one. The boundary between the two zones is horseshoe shaped. The lower zone is about 520 m long.

Open land mostly hayfields and pastures surround the landslide. The area inside the landslide scar is wooded in the southeast quadrant and pasture or wetland in other areas and does not appear to have been cultivated. The post failure terrain appears well preserved. The terrain outside the landslide zone also appears little altered by human activities (see LiDAR image in Fig. 1).

East of O'Conner Road, surface water discharges to a gully and flows eastward away from the landslide zone. The drainage pattern inside the landslide zone is westward to Stag Creek. The creek is about 5 m wide and about a meter deep. Spring run-off may temporarily elevate the creek level by about 1 to 2 m as observed from the bending pattern of the dead grass along the creek banks. The creek banks are mostly tree covered. The bank slopes are generally about 2.3H:1V, with the height ranging from 10 m to 35 m. Surface sloughing or small scale slope failures are visible from vegetation changes or freshly exposed soils. The creek is incised nearly to bedrock. Probing along the creek encountered bedrock at about 2 to 3 m depth at some locations. Large areas of horizontally bedded clay are visible along the creek. At some locations, the clays are exposed by some tens of meters along the creek bed.

Brooks (unpublished) identified a large landslide complex along Stag Creek that encompasses an area of about 10.1 km long by about 1.6 km wide and extends to both sides of the creek. The study landslide is inside the northern end of the complex. Available radiocarbon dates indicate that the large landslide complex is aged about 5200 cal yr BP although additional chronological evidence is required to confirm the hypothesis. Brooks (2015) attributed the complex to another major earthquake of 5200 cal yr BP evidenced from 13 landslides in the region.

3. FIELD AND LABORATORY TESTS

A geotechnical field program was carried out at the Low landslide site. The program started with micro-seismic surveys to determine the sediment thickness in and around the landslide zone. The survey was done with a handheld tri-axial seismograph (Tromino®) to measure the horizontal-to-vertical spectral ratio (HVSR) of the ambient noise in the ground. Correlations between the sediment thickness and HVSR by Hunter et al. (2010) and Crow et al. (2017) were used to calculate the sediment thickness. A total of 27 locations (Fig. 1) were surveyed with the instrument. The interpreted sediment thicknesses were used for planning of the subsequent field testing programs.

Cone Penetrometer Tests (CPT) were carried out at CPT1 to CPT4 as shown in Fig. 1. Field Vane Shear Tests (VST) were carried out at VST1 to VST4 that are adjacent to the CPT holes (Fig. 1). Table 1 provides coordinates and depth of each test hole.

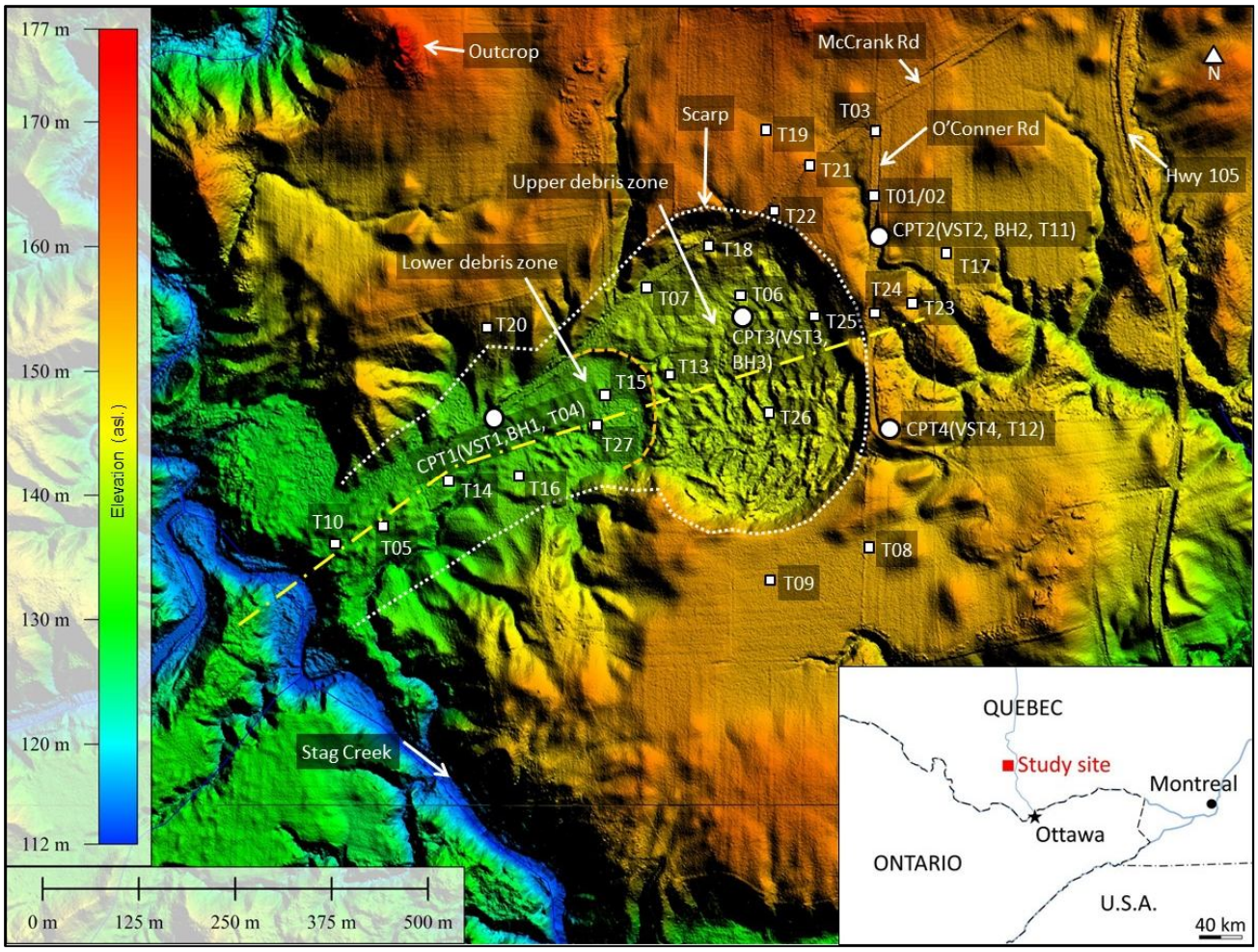

Fig. 1. Location map of study area (LiDAR image ©Government of Quebec). The white dotted line marks the perimeter of the large failure zone (likely the extent of a 5200 cal yr BP failure). The orange dashed line is the boundary between an upper debris plateau and a lower debris plateau (likely 1020 cal yr BP failure). The yellow dash-dotted line is the approximate centerline where slope stability is analyzed. The square dots are locations of micro-seismic surveys. The rounded dots are drill hole locations.

Table 1. CPT and VST location coordinates and total depths

Test Location	Coordinates	Depth of CPT (m)	Depth of VST (m)
CPT1, VST1	N45°49.633 W75°59.393	19.4	19.0
CPT2, VST2	N45°49.760 W75°59.011	36.0	36.0
CPT3, VST3	N45°49.701 W75°59.142	28.4	23.0
CPT4, VST4	N45°49.625 W75°58.996	42.7	24.0

The Cone Penetrometer Tests were conducted to determine the soil in-situ strength parameters. A commercial 30-ton truck mounted CPT rig was used for the tests. The rig was equipped with an integrated electronic piezocone penetrometer and data acquisition system. The cone had a maximum tip capacity of 37.5 MPa, a sleeve capacity of 1.0 MPa, and a pore pressure transducer capacity of 1.4 MPa. The cone was pushed to refusal (bedrock) at all four test locations.

The field Vane Shear Tests were carried out with a portable Nilcon Vane Borer (RocTest M-1000). The purpose is to determine the in-situ undrained shear strength of the clay and for calibration of the CPT data. The equipment consists of a torque recording head, boring rods, various sized vanes and a slip coupler. During testing, the torque is scribed on a waxed paper disc mounted inside the torque head. The slip coupler installed between the vane and rod allows a free slip of 15º before the vane is engaged. The torque recorded during the free slip reflects the rod friction that is subtracted from the subsequent reading for net shear resistance of the soil.

Soil samples were collected at BH1, BH2 and BH3 (next to CPT1, CPT2 and CPT3 respectively) with thin wall aluminum tubes of 38 and 48 mm diameter. A portable auger was used to pre-drill the holes before coring. The samples were taken from depth ranging from 2.6 m to a maximum of 23 m below surface. The sample tubes were sealed with plastic caps and electrical tape and stored in a fridge until extruded for laboratory testing immediately after the sampling program. The samples were tested for geotechnical index properties at the Sedimentology Laboratory of the Geological Survey of Canada.

4. TEST RESULTS AND INTERPRETATION

The results of the sediment thickness interpreted from the micro-seismic surveys are provided in Table 2. The CPT depths to refusal are also shown in this table for comparison. Clearly, the micro-seismic survey results reflect the actual sediment thickness fairly well at the CPT locations. The discrepancy ranges from 0 to 5 m, which is within the expected error margin. The largest deviation is 5 m between T04 and CPT1. Bedrock slope is expected at this location that might have led to the discrepancy. Nevertheless, the sediment thickness surveyed with the geophysics instrument was useful for the purpose of this study.

The soil gradation and other index properties obtained from the laboratory tests are provided in Figs. 2 and 3 as well as in Table 3. As seen in Fig. 2, the materials tested are silty-clay or clayey-silt. Higher plasticity was observed at shallower depths as shown in Fig. 3 and Table 3.

The field Vane Shear Test results of the peak undrained shear strength (C_u), remoulded shear strength (C_r) and sensitivity (S_t) are provided in Fig. 4. The ranges of the strength and sensitivity values are listed in Table 4.

The CPT results of the peak undrained shear strength were calculated from the CPT corrected tip resistance (q_t) and the overburden pressure (σ_{vo}) with a bearing factor N_{kt} as: $C_u = (q_t - \sigma_{vo}) / N_{kt}$ (Konrad and Law, 1987; Yu and Mitchell, 1998). The N_{kt} factor was calibrated with the VST data. The C_u results are shown in Fig. 5. A factor of $N_{kt} = 17.0$ was obtained for the undisturbed clay at CPT2 and CPT4. However, CPT1 yielded $N_{kt} = 11.5$, which is inside the landslide zone. At CPT3, $N_{kt} = 11.5$ was obtained above elevation 134 m and $N_{kt} = 17.0$ below elevation 134 m. Note that the water table (phreatic surface) at CPT3 is about 133 m above sea level (Fig. 5). The water table coincides with the elevation where the N_{kt} value changes. From the N_{kt} perspective, the materials above 134 m asl. at

CPT3 exhibits the characteristics similar to that of CPT1 (in disturbed area). The materials below 134 m asl. behave similarly to that of CPT2 and CPT4 (in undisturbed area). In other words, the materials above 134 m asl. at CPT3 are likely disturbed by the landslide and the lower part is likely not. The sudden change of the CPT profile at elevation 133 m also indicates that a shear band is likely located at the vicinity of elevation 133 m to 134 m.

Table 2. Results of micro-seismic survey of sediment thickness and CPT confirmation

Survey location #	Seismic survey (m)	CPT refusal (m)	Survey location #	Seismic survey (m)	CPT refusal (m)
T01/02	25		T15	26	
T03	21		T16	14	
T04	24	19 (CPT1)	T17	26	
T05	17		T18	27	
T06	28	28 (CPT3)	T19	11	
T07	19		T20	10	
T08	30		T21	29	
T09	18		T22	28(?)	
T10	18		T23	39	
T11	33	36 (CPT2)	T24	39	
T12	44	43 (CPT4)	T25	39(?)	
T13	27		T26	36	
T14	22		T27	27	

Table 3. Geotechnical index properties of soil samples

Bore hole #	Depth (m)	Elevation asl. (m)	Water content W_c (%)	Plastic limit PL (%)	Liquid limit LL (%)	Plasticity index I_p (%)	Liquidity index I_L	Unit weight γ (kN/m^3)	Specific gravity G_s
BH1	3.0	132.4	57.7	23.9	55.2	31.3	1.08	16.2	2.79
	4.0	131.4	55.9	23.8	55.9	32.1	1.00	16.9	2.79
	5.0	130.4	54.7	23.6	65.7	31.1	1.00	16.8	2.79
BH2	5.1	147.3	56.1	37.2	71.4	34.2	0.55	16.1	2.81
	7.1	145.3	57.7	34.8	75.3	40.5	0.57	16.3	2.81
	9.2	143.2	54.3	37.5	73.7	36.2	0.46	16.2	2.81
	11.1	141.3	49.9	30.9	60.3	29.4	0.65	16.5	2.80
	13.2	139.2	40.3	27.8	51.9	24.1	0.52	17.4	2.79
	15.2	137.2	52.5	29.8	48.2	18.4	1.23	16.6	2.81
	17.2	135.2	40.6	26.8	43.8	17.0	0.81	17.2	2.80
	19.1	133.3	49.7	21.3	33.0	11.7	2.44	17.2	2.80
	20.1	132.3	50.4	26.1	40.9	14.8	1.64	16.8	2.81
	22.1	130.3	46.1	21.6	32.0	10.4	2.36	17.3	2.81
BH3	2.6	140.0	52.0	31.3	61.2	30.0	0.69	16.7	2.78
	6.8	135.8	52.9	31.6	66.7	35.2	0.61	16.4	2.80
	7.9	134.7	42.1	21.8	36.3	14.5	1.40	17.2	2.79
	9.1	133.5	45.6	27.4	40.6	13.3	1.38	17.1	2.80
	10.1	132.6	52.2	21.3	32.0	10.7	2.89	17.3	2.79
	12.3	130.3	36.5	24.7	38.3	13.7	0.86	17.4	2.78
	14.2	128.4	38.8	24.5	36.0	11.5	1.25	17.6	2.79

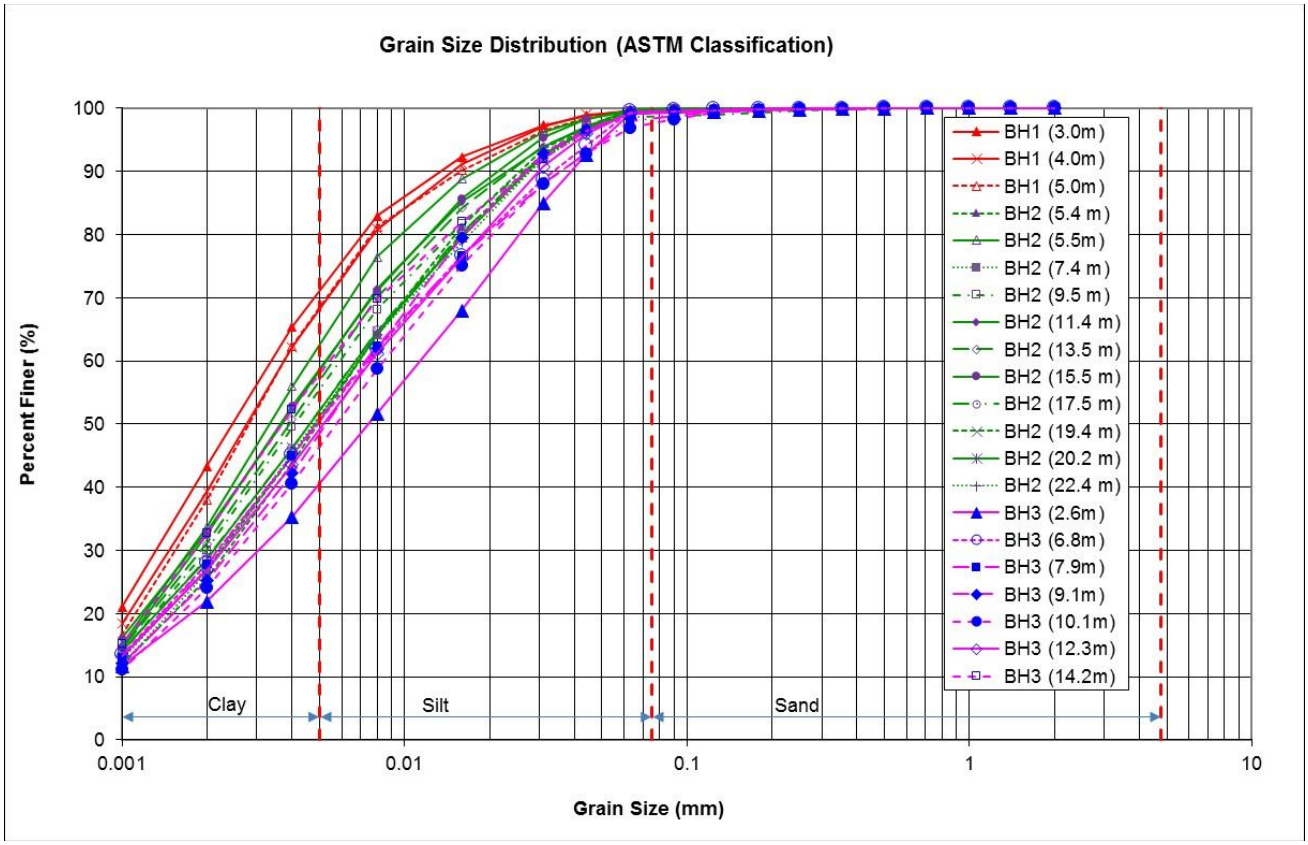

Fig. 2. Gradation chart of soil samples

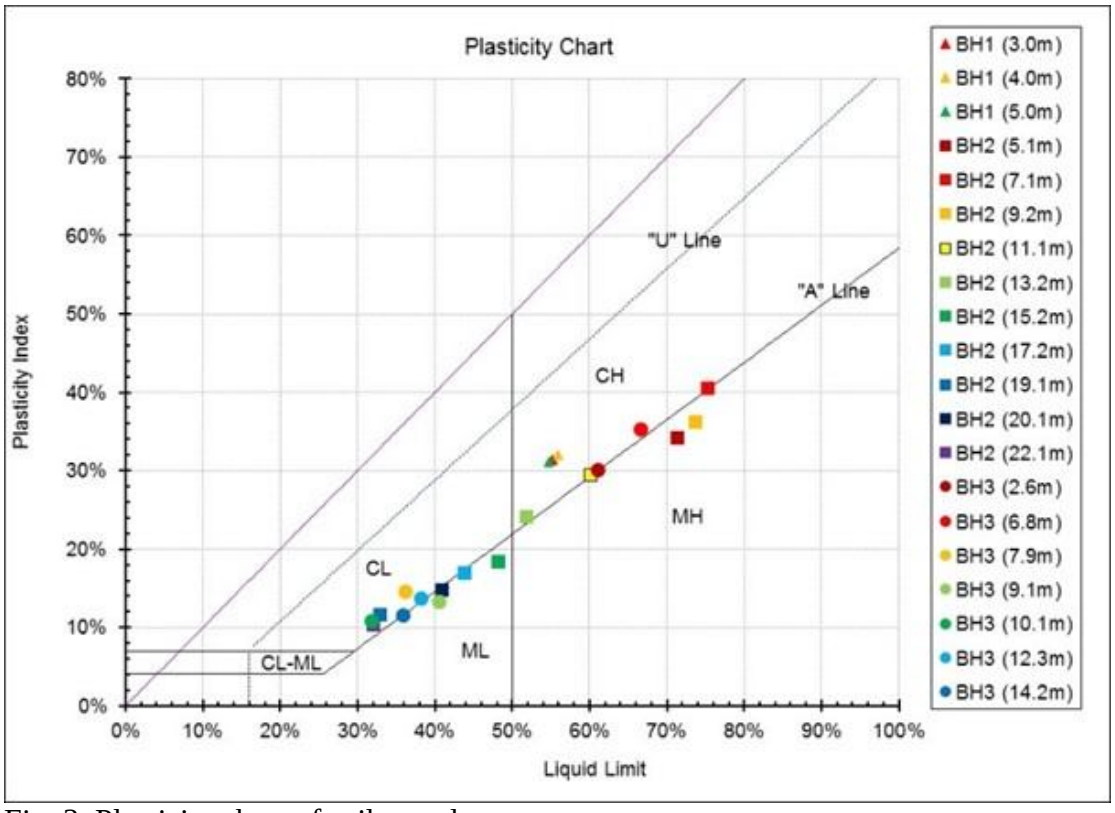

Fig. 3. Plasticity chart of soil samples

The C_u results were also calculated from the excess pore pressure behind the cone tip (Δu) by $C_u = \Delta u / N_{\Delta u}$ where $N_{\Delta u}$ is a pore water bearing factor (Tavenas and Leroueil, 1987). However, the two bearing factors, N_{kt} and $N_{\Delta u}$, are interrelated as $N_{\Delta u} = B_q \cdot N_{kt}$, where B_q is pore pressure parameter calculated as $B_q = \Delta u/(q_t - \sigma_{vo})$. The B_q values vary with location and depth. The calculated B_q profiles at all the CPT locations are shown in Fig. 6. The approximate average B_q values below the surface crust are 0.83, 0.97, 0.84, and 0.97 for CPT1, CPT2, CPT3, and CPT4 respectively. With the N_{kt} values discussed above, the corresponding $N_{\Delta u}$ values were calculated to be 9.5, 16.5, 14.3, and 16.5 for the materials below the phreatic line at CPT1, CPT2, CPT3, and CPT4 respectively. The C_u results calculated from $N_{\Delta u}$ are also plotted in Fig. 5. As seen from this figure, the C_u results from $N_{\Delta u}$ and N_{kt} agree well (below phreatic surface) at all CPT locations.

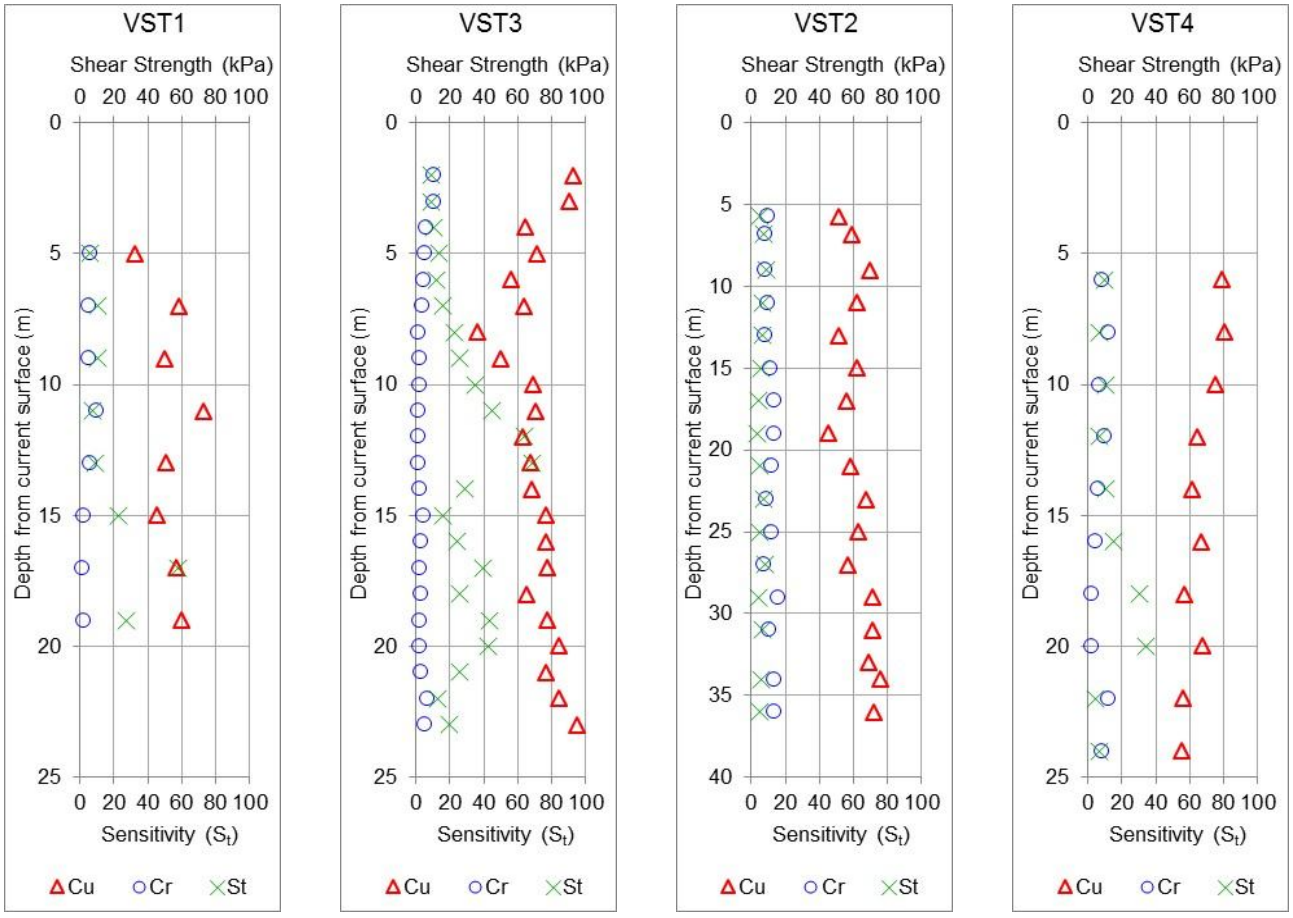

Fig. 4. Vane Shear Test results (C_u = peak undrained shear strength; C_r = remoulded shear strength; S_t = sensitivity)

Table 4. Ranges of VST results

Location	C_u (kPa)	C_r (kPa)	S_t
VST1	32 ~ 73	1 ~ 10	6 ~ 58
VST2	45 ~ 76	7 ~ 16	3 ~ 9
VST3	36 ~ 95	1 ~ 11	9 ~ 68
VST4	55 ~ 81	2 ~ 12	5 ~ 34

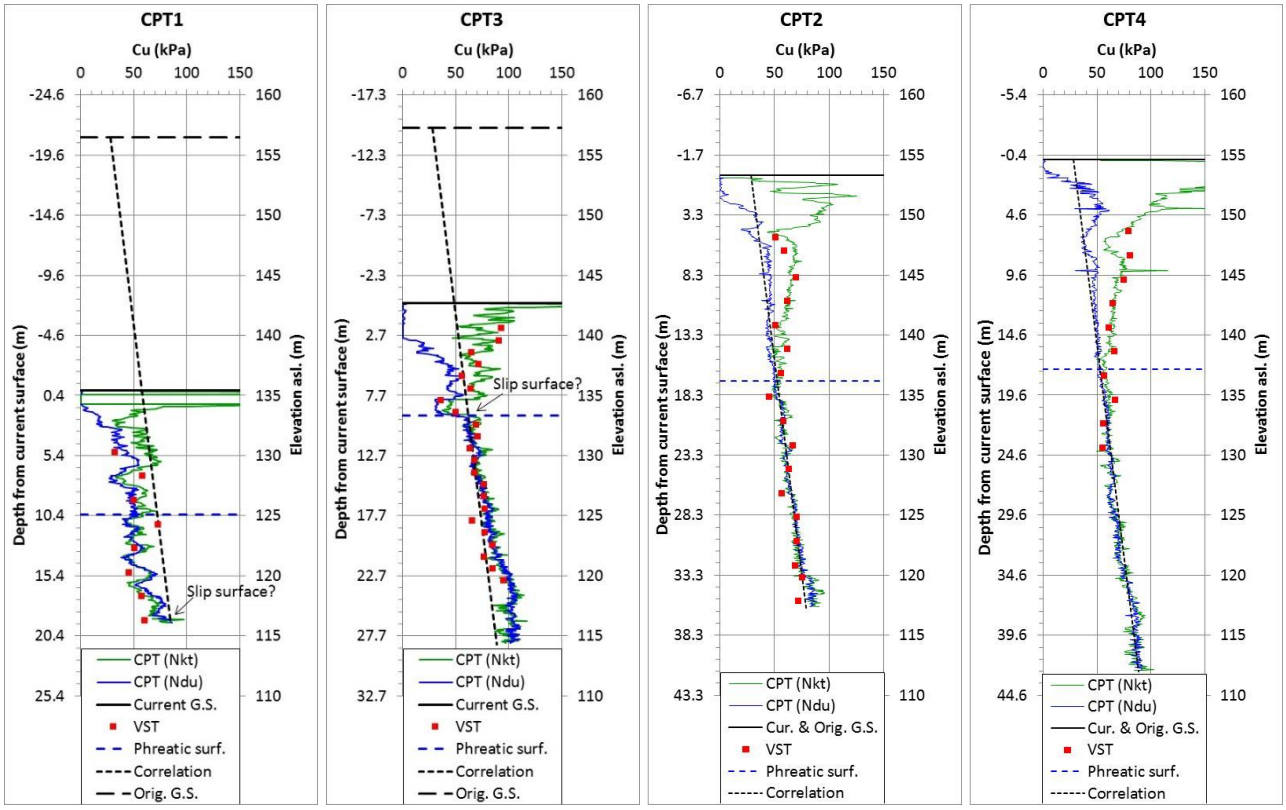

Fig. 5. CPT peak undrained shear strength (C_u) calibrated with VST results (All CPT's stopped at depth of refusal)

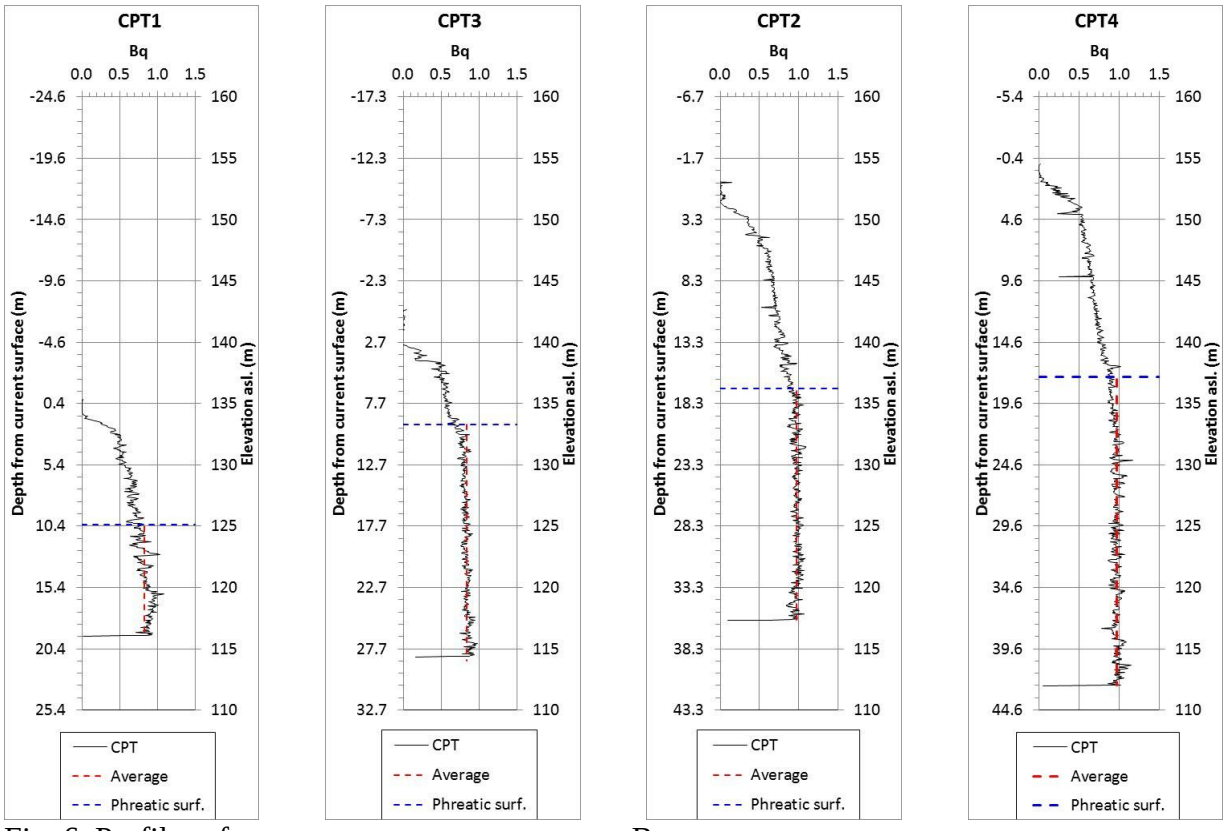

Fig. 6. Profiles of pore water pressure parameter B_q

The pre-failure ground surface at CPT1 and CPT3 are inferred from the adjacent terrain undisturbed by the landslide (Fig. 1). The surfaces at CPT2 and CPT4 are not affected by the landslide. The interpreted pre-failure ground surface and the current surface at all CPT locations are shown in Fig. 5. By comparing the CPT results in Fig. 5, it was found that the C_u profiles at CPT2 and CPT4 follow the same trendline for the sediment below phreatic surface, which is:

$$C_u = 28 + 1.42\ H \qquad [1]$$

where C_u = peak undrained shear strength (kPa); and H = depth (m) from the pre-failure ground surface.

It is noted that the C_u profile of CPT3 follows approximately the same correlation expressed in eq. [1] for the portion below the phreatic line. This is another indication that the materials below the phreatic line at CPT3 are not affected by the landslide. A sudden drop of C_u occurred at elevation 133 m to 134 m as seen on the CPT3 chart. This feature is not observed at CPT2 or CPT4 where the sediments are not affected by the landslide. The weakened layer of material is likely relocated to here at CPT3 from an upper elevation. This is another indication that the slip surface is likely at 133 ~ 134 m elevation and coincides with the water table.

As shown in Fig. 5, the C_u profile at CPT1 deviates entirely from the trendline (eq. 1). The materials at this location exhibit lower shear strength than the trendline. There are two possible explanations for the deviation: (1) The materials at CPT1 were relocated from an upper elevation. In other words, the landslide slip surface could be near the bedrock. (2) The original Champlain Sea plain at CPT1 was much lower than that shown in Fig. 5. Note that the C_u profile of CPT1 "swings" considerably. The irregularity of the C_u profile is not consistent with that of the undisturbed clay at other locations (CPT2 and CPT4). It is therefore believed that explanation (1) above is more likely the case, i.e., the slip surface is located near bedrock at CPT1.

5. SLOPE FAILURE MECHANISM

5.1 Cause of Two Debris Plateaus

Brooks (unpublished) discovered two distinct layers of buried soil-organics at the toe of the landslide. The materials were exposed along the east bank slope of Stag Creek. Radiocarbon dates unveiled two layers of debris deposits: a lower layer about 5200 cal yr BP and an upper layer about 1020 cal yr BP. Brooks (2014a, 2014b and 2015) referred to the two ages as added evidence of two earthquakes that are responsible for a total of 13 and 12 landslides aged 5200 and 1020 cal yr BP respectively in the general Ottawa-Gatineau region. As mentioned earlier, he initially thought that the large elongated 790 m x 430 m scar (Fig. 1) was one failure of 1020 cal yr BP. The origin of the 5200 cal yr BP debris layer was yet to be explained. The information from the current geotechnical investigation sheds light on understanding the source of the two debris layers.

As pointed out earlier, there are two distinct debris plateaus inside the landslide scar. A cross-section along the approximate centerline of the landslide (See Fig. 1 for location) is shown in Fig. 7. The two plateau surfaces are approximately parallel to each other. The downstream plateau is about 5 m lower than the upper one. By extrapolating the upper plateau surface towards the creek, it appears that the

drop of the lower debris zone is unlikely a local variation of a single failure. Rather, it is more likely the result of two staged failures. The lower debris zone is likely the result of a second failure inside the larger failure occurred earlier.

One argument against the two staged failure hypothesis is that bedrock change may have caused stepped debris surface of one failure. However, the micro-seismic survey and drillhole results indicate that the bedrock surface is relatively level across the entire section as shown in Fig. 7 (note 4 times exaggeration of the vertical scale). No obvious bedrock feature suggests any major influence on the stepped debris surface.

Another argument could be that stepped slip surface may have developed causing the drop of the debris plateau. An example is the Notre-Dame-de-La-Salette landslide reported by Perret et al. (2013). The landslide was triggered by an earthquake in 2010. Two plateaus of debris surface developed similar to that of the Low landslide. The elevation difference between the two plateaus is about 3 m. Drillhole information unveiled two stepped slip surfaces corresponding to the two plateaus. The lower zone failed at a depth about 8 m below that of the upper zone. Even though the deeper failure created a lower plateau on the surface, the elevation change between the two plateaus is gradual indicating a continuous flow transition. The transition zone forms more or less a straight bench across the landslide from one side to the other. Whereas at the Low landslide, the boundary between the two debris plateaus is semi-circular. The face of the bench slope at the Low site is fairly sharply visible with its crest and toe easily discernable both on the LiDAR image (Fig. 1) and on site. This is despite that the landslide is over a thousand years old. The features clearly indicate a fresh shear failure (instead of a continuous flow transition) that is typically observed at the head-scarps of sensitive clay landslides.

It is common understanding that the slip surface of sensitive clay failures tends to follow the weak bedding planes of the sediments (e.g., Odenstad 1951, Bjerrum 1955, Carson 1977, Locat et al. 2011 and Quinn et al. 2011), which are usually sub-parallel to the surface of the sediments. As seen in Fig. 7, the two debris plateaus are not only subparallel to each other, but also to the interpreted pre-failure Champlain Sea surface. The CPT measurements indicate an almost perfectly linear groundwater table as shown in Fig. 7. The groundwater table is also sub-parallel to the original ground surface. As Bjerrum (1955) noted, the lowest shear strength of sensitive clays is often just below the drying crust that forms the most dangerous sliding surface parallel to the surface of the slope. The sediments at the study site is no exception as seen from Fig. 5. As discussed earlier, the depth of failure at CPT3 coincides with the water table. Along with the sediment bedding plane, the ground water table might also have contributed to the potential shear plane. By projecting the depth of failure from CPT3 and following the groundwater table, a slip surface could be interpreted to intercept the projected shear plane at the headscarp and exit at the stream valley side slope as shown in Fig. 7. This slip surface may represent the first stage failure. The depth of failure at CPT1 discussed earlier may help delineate another slip surface in the same manner as shown in Fig. 7. This may represent a second stage failure inside the earlier debris zone. This interpretation might help explain the two aged debris layers discovered by Brooks (unpublished). The debris from the first failure tumbled down and the organic layer was buried about 5200 cal yr BP. Since then, vegetation had regrown over the next four thousand years. When the next earthquake struck about 1020 cal yr BP, the second failure occurred. The debris flowed down and the newer surface organic layer was deposited above the older layer. It should be noted that, although this interpretation is reasonable based on the available data, further radiocarbon dating inside the landslide scar should help establish more definitively the age of the two failure zones.

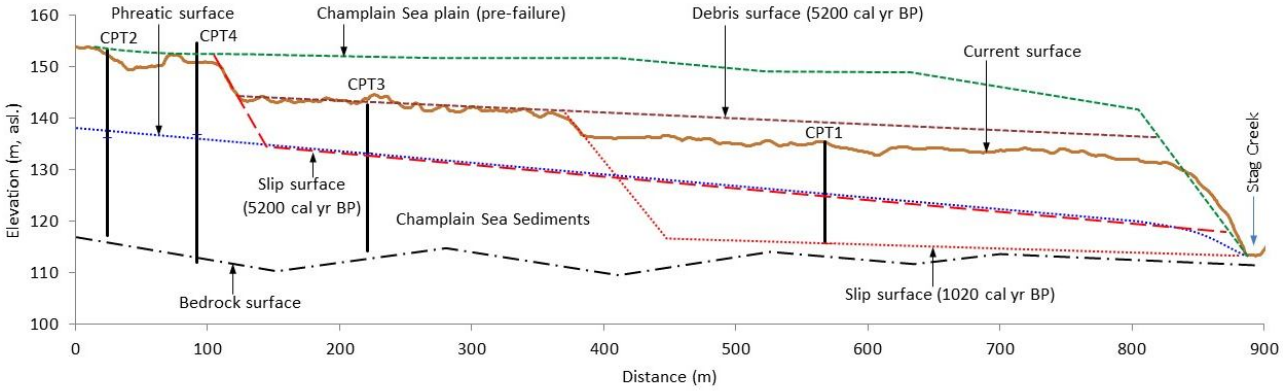

Fig. 7. Cross-section of the landslide (location shown in Fig. 1). The CPT locations are approximate projections to the centerline. (Vertical exaggeration: 4x)

5.2 Flake Type Failure

Champlain Sea clay landslides are well known for their retrogressive failure behavior. Whether the Low landslide of 1020 cal yr BP is another retrogressive failure is a question that affects how much ground acceleration is required to trigger the failure.

Mitchell and Markell (1974) compiled data from 75 sensitive clay landslides that exhibit a correlation between a stability number and retrogression distance. The stability number (N_s) is defined as:

$$N_s = \gamma H / C_u \qquad [2]$$

where γ is soil unit weight; H is height of slope; and C_u is soil peak undrained shear strength.

At the Low landslide site, the average unit weight is $\gamma = 16.8$ kN/m^3 (Table 3). The height of the slope prior to the 1020 cal yr BP failure is about H = 22 m. The peak undrained shear strength is calculated from eq. [1] to be $C_u = 73.4$ kPa (with reference to the original Champlain Sea surface). The estimated stability number is therefore $N_s = 5.0$. According to Mitchell and Markell (1974), the retrogression distance with $N_s = 5.0$ is 82 m. The 1020 cal yr BP failure occurred to a distance of 520 m, or more than 6 times the predicted distance. Based on this criterion, the landslide could not have failed retrogressively.

Zhang et al. (2018) reported a numerical study of retrogressive failures with emphasis on the role of clay sensitivity. The results show a strong correlation between landslide retrogression distance and clay sensitivity. Note in Fig. 4 that the sensitivities of the clay unaffected by the landslide (VST2, VST4, and lower portion of VST3) are mostly from 5 to 40 (except for a couple of extreme readings). With this sensitivity range, the correlation by Zhang et al. (2018) predicts a retrogression distance of 78 m to 217 m (average 148 m). It is much shorter than the actual 520 m length of the scar. This is another indication that the 1020 cal yr BP landslide is unlikely a retrogressive failure.

The Low landslide has similarities to the Breckenridge landslide studied as part of this overall paleoseismicity investigation. Wang (2018) presents a number of evidences and concluded that the

study landslide of 980 m long at Breckenridge is a flake slide (a slip surface initiated along the overall slope at the onset of the failure, Bjerrum 1973). Among the evidences are 36 other modern to ancient landslides in the Breckenridge area. All the 36 landslides failed into small creeks that are similar to the Stag Creek at the Low site. The lengths of the 36 landslides range from 70 m to 370 m (average 220 m). One of them is a well-documented landslide of 1963 that retrogressed a distance of 140 m. The failure process of the other landslides are unknown, but many if not most of them must be retrogressive. Assuming they are all retrogressive (conservative for this discussion), the failure distances are limited to only 70~370 m. The reason for the relatively short retrogression distance is believed to be limited by the small capacity of the creeks to accommodate the debris or to discharge the debris quickly. The debris mounted-up quickly in the flow channel and buttressed the slope that prevented the failure from retrogressing a long distance. The much longer failure distance of the study landslide at Breckenridge can only be explained by flake slide. The material properties at the Low site are similar to that at the Breckenridge site. The stability number for the Breckenridge landslide is $N_s = 4.0$, while for the Low site $N_s = 5.0$ as discussed above. Therefore, it is likely that the Low landslide is also a flake type failure.

Eden et al. (1971) documented a large retrogressive landslide at the South Nation River about 48 km east of Ottawa in 1971. The failure occurred in Champlain Sea clay following a heavy rainstorm. The failed valley side was about 24 m high. The head scarp extended landward to about 490 m from the river. The debris flowed both upstream and downstream of the river filling about 2.5 km of riverbed, and raising the river level by more than 11 m before it overtopped.

Evans and Brooks (1994) described another retrogressive landslide along the South Nation River at Lemieux in 1993. It was about 4.5 km downstream of the 1971 landslide. The trigger is believed to be related to wet spring conditions. The landslide started from a valley side of about 23 m high. The average depth of failure is about 18 m. A debris plug, about 12 m high and 3.3 km long dammed the river. The head scarp retrogressed by about 680 m inland.

Eden et al. (1971) quoted some average material properties of nearby sites from other sources. Evans and Brooks (1994) also quoted some material properties from other sources for the Lemieux landslide site. The average values of those data are listed in Table 5. Although details are not available, the data do show similarities to those in Tables 3 and 4 for the Low site.

Table 5. Material properties at the South Nation River and Lemieux landslide sites

Site	Depth (m)	W_c (%)	PL (%)	LL (%)	I_P (%)	I_L	γ (kN/m^3)	C_u (kPa)	C_r (kPa)	S_t	Reference
S. Nation R.	-	70	30	70	40*	1.0*	15.7	49	-	10-100	Eden et al. (1971)
Lemieux	8-32	36.4-59	19.9-27.8	31.4-56.2	19.9*	0.8-1.6	-	41.7-76.7	3.7-10.9	4.3-11.4	Evans & Brooks (1994)

Note: * Calculated based on average values of reported Atterberg limits; W_c = water contents; PL = plastic limit; LL = liquid limit; I_P = plasticity index; I_L = liquidity index; γ = unit weight; G_s = specific gravity.

Evans and Brooks (1994) reported a stability number of $N_s = 9.6$ for the 1993 Lemieux landslide. With this stability number, Mitchell and Markell (1974) correlation predicts a retrogression distance of 723 m, which agrees well with the actual 680 m measurement at the Lemieux site. This is an indirect validation of Mitchell and Markell (1974) prediction for the Low site discussed earlier. By applying the sensitivity values of 4.3-11.4 quoted for Lemieux (Table 5) to Zhang et al. (2018) correlation, the predicted retrogression distance is only 73-142 m that is substantially smaller than the actual 680 m measurement at Lemieux. Note that Eden et al. (1971) quoted a much higher sensitivity range of 10 to

100, which might be more reasonable given the proximity between the two landslide sites. However, it is difficult to compare the clay sensitivity without detailed information.

Qualitatively, the descriptions of the South Nation River and Lemieux landslides provide insight into understanding the Low landslide. The above two landslides along the South Nation River are relatively large among the well documented Champlain Sea clay failures in the region. Based on the descriptions, the debris plugs must have played a key role in stopping the failure from retrogressing further. In other words, the debris buildup in the river buttressed the toe and stabilized the slope. There is no doubt that the height of the debris plug depends on the volume of debris generated and the volume capacity of the river channel. The average width of the South Nation River is about 50 m (Evans and Brooks 1994). The water flow at the Stag Creek is only 5 meters wide (and often narrower depending on location). The volume capacity of the river is much larger than the creek. It is therefore much easier for the creek to be plugged by landslide debris than for the river. However, the Low landslide failed to a distance similar to those at the South Nation River. This is another indication that the Low landslide may well be a flake type failure instead of a retrogressive process.

Furthermore, as discussed earlier, the 1020 cal yr BP failure likely occurred inside the debris zone of the older failure. Generally, the overall shear strength of the debris deposit should be enhanced. This is because the sensitive clays are mixed with the surficial materials that are typically coarser. Not only has the debris matrix become stronger, but also less sensitive. The debris deposit may less likely fail retrogressively than for the pure sensitive clays. Note from Fig. 7 that the upper debris plateau (the older failure) is about 10 m below the original Champlain Sea plain. The lower plateau (the younger failure) is only about 5 m below its pre-failure surface. The volume ratio of material disappeared from the second failure is less than that of the first failure. This may have been attributed to the lower sensitivity of the debris mixture than that of the undisturbed clay. Not only does this support the argument of a non-retrogressive failure, but also provide an added evidence to the two-staged failure hypothesis discussed earlier.

In summary, the 1020 cal yr BP landslide is most likely a flake slide, i.e., an initial slip surface developed to the full extent of the landslide zone at the onset of the failure.

6. SLOPE STABILITY ANALYSIS

The stability of the reconstructed slope discussed earlier is analyzed to estimate the threshold ground acceleration required to trigger the failure. There are various types of models available for slope stability analysis. They range from a simple closed form solution, limit equilibrium methods, finite element, discrete element and coupled methods. Some models can simulate material flow process, e.g., Roy and Hawlayder (2017). However, the most sophisticated models are not without serious limitations. For example, the material parameters cannot be easily acquired and there is lack of standard of acquiring them. The assumptions made at microscopic level, e.g. particles and their interactions for some latest models still have considerable room for improvement. The analysis in the current study uses a limit equilibrium model that is considered appropriate. Limit equilibrium models are the most widely used and tested methods that calculate the factor of safety by comparing soil resistance with driving force. The calculations are straight forward and the required parameters can be obtained with well established and standardized methods. Although its simplicity comes with limitations that encourage development of alternative tools, its rich case history and proven success rate justify its use for the purpose of this study.

A two-dimensional limit equilibrium model, Slope/W developed by Geo-Slope International (2010) is used in this study. Slope/W is an industry standard software that has been widely used internationally for slope stability design. The model is well suited for translational slope failures as the case here in this study.

The cross-section shown in Fig. 7 is analyzed with Slope/W. The ground surface prior to the 1020 cal yr BP failure is assumed by extrapolating the upper debris plateau (Fig. 8). The geometry of the pre-failure creek bank slope is extrapolated from the current bank slope. The sensitivity of this assumption diminishes with the relatively long slope. The slip surface is inferred as discussed earlier. One soil unit is assumed overlying bedrock in the model. The hardened surface crust has negligible effect due to the great length of the slope and is therefore ignored for simplicity. The peak undrained shear strength given by Eq. [1] is used in the analysis. For the purpose of calculating the shear strength, the original Champlain Sea surface is used as a reference, which is assumed to be 10 m above the debris surface of the previous failure. A unit weight of 16.8 kN/m^3 is assumed based on the average test result in Table 3.

Pseudo-static total stress analysis is performed with the Morgenstern-Price method (Verification with other methods resulted in very marginal differences). A horizontal seismic coefficient is applied to the model and the vertical seismic load is ignored as it has negligible effect on the relatively flat ground. The analysis is performed with a trial-and-error approach. A random seismic coefficient is applied to the model and its corresponding Factor of Safety (FOS) is calculated. The coefficient is then adjusted for another calculation and the cycle repeats until a FOS = 1.0 is achieved, which is considered as a critical condition. A threshold seismic coefficient of 0.19 g is obtained to achieve FOS = 1.0.

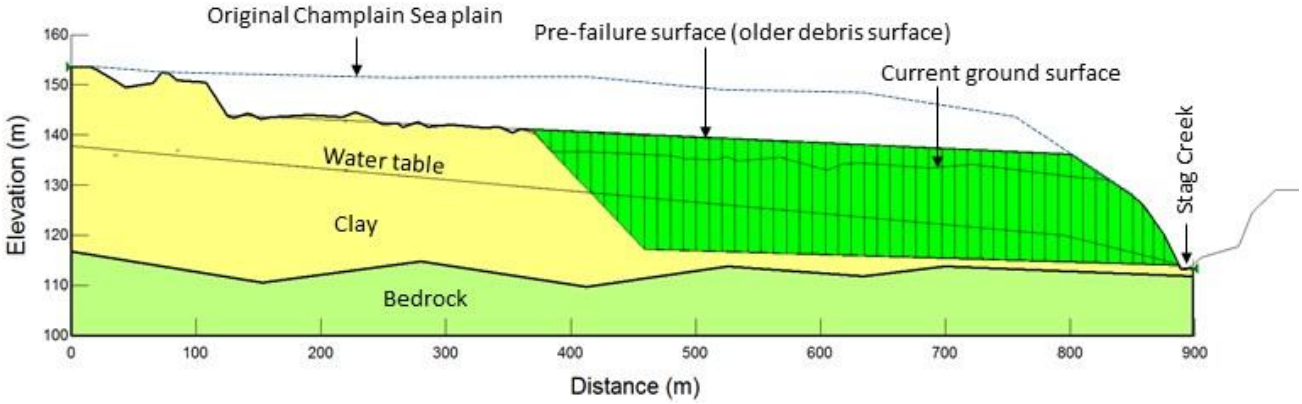

Fig. 8. Slope/W model (sliding body shaded in green) (Vertical exaggeration: 4x)

7. DISCUSSION

The Low landslide is one of three landslides studied for the purpose of further understanding the 1020 cal yr BP earthquake in the Ottawa-Gatineau region. The studies of the other two landslides: one at Quyon and the other at Breckenridge, Quebec, are reported by Wang (2016) and Wang (2018) respectively. The Quyon site is about 37 km southwest of the Low site. The Breckenridge site is about 38 km south-southeast of the Low site. The distance between Quyon and Breckenridge sites is about 30 km. The threshold horizontal ground accelerations at Quyon and Breckenridge are estimated to be 0.28 g and 0.27 g respectively. The result, 0.19 g, at the Low site is lower than those of the other two sites. This is consistent with other observations.

Among the 12 landslides of 1020 cal yr BP identified by Brooks (2015), nine of them are clustered around and between Quyon and Breckenridge. Only one other landslide was identified near Low, which is located at Mullin Creek, Quebec, or about half way between Low and Breckenridge (Brooks, unpublished). Although dating of ancient landslides cannot be exhaustive, the more failures found closer to Quyon and Breckenridge as well as the much large size of the two landslides are indications that the ground shaking was more intense at Quyon and Breckenridge than at Low.

The result from this study is also comparable to a recent event in the region. An earthquake occurred at Val-des-Bois, Quebec on June 23, 2010. The epicenter is located at about 40 km east-northeast of the Low landslide site. Atkinson and Assatourians (2010) and Lin and Adams (2010) reported earthquake moment magnitude M_w 5.0 for this event. Ma and Motazedian (2012) later indicated a moment magnitude of M_w 5.2. Lin and Adams (2010) reported a horizontal peak ground acceleration of 0.15 g recorded at a soil site about 49 km away from the epicenter. The 2010 earthquake is known to have triggered two Champlain Sea clay landslides about 12 km and 18 km away from the epicenter (Perret et al. 2013). The sizes of the landslides are 420 m x 150 m and 80 m x 180 m. While the epicenter and magnitude of the 1020 cal yr BP earthquake are yet to be analyzed and presented separately, the minimum horizontal ground acceleration of 0.19 g calculated from the Low landslide seems reasonable when compared to the recent record.

8. CONCLUSION

The peak undrained shear strength (C_u) of the Champlain Sea clay at the Low landslide site ranged from 32 to 95 kPa from four vane shear test holes at 2 m to 36 m depth range. The remoulded shear strength ranged from 1 to 16 kPa, and sensitivity from 3 to 68. The CPT cone tip bearing factor, N_{kt}, was calculated as 17.0 for the clay undisturbed by the landslide and 11.5 for the disturbed materials. The CPT pore water bearing factor $N_{\Delta u}$ varied with location. A correlation of the C_u profile was found to be $C_u = 28 + 1.42$ H, where H is depth in meters from the pre-failure ground surface (original Champlain Sea plain). The large landslide scar is likely a product of two failures, one about 5200 cal yr BP and another about 1020 cal yr BP. The newer failure occurred inside the older failure zone and its slip surface is deeper than the previous failure. A horizontal ground acceleration responsible for the 1020 cal yr BP failure is estimated to be a minimum of 0.19 g.

ACKNOWLEDGEMENT

The author would like to thank Alain Grenier and Jeremie Rivest for their assistance with field works. Greg Brooks kindly provided his insight and knowledge about the study area. Review and comments from Ted Lawrence on the field and laboratory test results are much appreciated. Kind review of the manuscript by Miroslav Nastev is also appreciated. This paper is a product of the Earthquake Geohazard Project, Public Safety Geoscience Program of Natural Resources Canada.

REFERENCE

Atkinson, G.M., Assatourians, K. 2010. Attenuation and source characteristics of the June 23, 2010 M5.0 Val-des-Bois, Quebec earthquake. Seismological Research Letters 81(5):849-860.

Bjerrum, L. 1955. Stability of natural slopes in quick clay. Géotechnique V:101-119.

Bjerrum, L., 1973. Problems of soil mechanics and construction on soft clays and structurally unstable soils (collapsible, expansive and others). State-of-the-art Report to Session 4, Proc. 8th ICSMFE, 3:111-159, Moscow, 1973. Also publi. in: Norw. Geotechn. Inst., Publ. 100.

Brooks, G.R., 2013. A massive sensitive clay landslide, Quyon Valley, southwestern Quebec, Canada, and evidence for a paleoearthquake triggering mechanism. Quaternary Research, 80, 425-434.

Brooks, G.R., 2014a. The age of sensitive clay landslides along the Gatineau Valley, SW Quebec, and their relationship to paleoseismicity in the West Quebec Seismic Zone; 2014 Eastern Section-SSA Meeting Report, Seismological Research Letters, 86(2A), DOI: 10.1785/0220150009.

Brooks, G.R., 2014b. Prehistoric sensitive clay landslides and paleoseismicity in the Ottawa Valley, Canada. In J.-S. L'Heureux et al. (eds.), Landslides in Sensitive Clays: From Geosciences to Risk Management, Advances in Natural and Technological Hazards Research 36, DOI 10.1007/978-94-007-7079-9_10, pp. 119-131.

Brooks, G.R., 2015. Evidence of paleoseismicity within the West Quebec Seismic Zone, eastern Canada, from the age and morphology of sensitive clay landslides. Proceedings of the 6th International INQUA Meeting on Paleoseismology, Active Tectonics and Archaeoseismology, 19-24 Apr. 2015, Pescina, Fucino Basin, Italy. 59-62.

Carson, M.A.1977. On the retrogression of landslides in sensitive muddy sediments. Can. Geot. J. 14:582-602.

Crow, H., S. Alpay, M. Hinton, R. Knight, G. Oldenborger, J.P. Percival, A. J.-M. Pugin, P. Pelchat, 2017. Geophysical, geotechnical, geochemical, and mineralogical datasets collected in Champlain Sea sediments in the Municipality of Pontiac, Québec. Geological Survey of Canada Open File 7881, 44 pages.

Eden, W.J., Fletcher EB, Mitchell RJ, 1971. South Nation River landslide, 16 May 1971. Can. Geot. J. 8:446-451.

Evans, S.G., Brooks G.R., 1994. An earthflow in sensitive Champlain Sea sediments at Lemieux, Ontario, June 20, 2993, and its impact on the South Nation River. Can. Geot. J. 31:384-394.

Geo-Slope International Ltd. (2010) Stability Modeling with Slope/W 2007 Version – An Engineering Methodology, Fourth Edition. 367 p.

Hunter, J. A., H. Crow, G. R. Brooks, M. Pyne, M. Lamontagne, A. Pugin, S. E. Pullan, T. Cartwright, M. Douma, R. A. Burns, R. L. Good, D. Motazedian, K. Kaheshi-Banab, R. Caron, M. Kolaj, I. Folahan, L. Dixon, K. Dion, A. Duxbury, A. Landriault, V. Ter-Emmanuil, A. Jones, G. Plastow, and D. Muir, 2010. Seismic site classification and site period mapping in the Ottawa area using geophysical methods, Geological Survey of Canada, Open File Report No. 6273. 80 pages.

Keefer, D.K. 1984. Landslides caused by earthquakes. Geological Society of America Bulletin 95: 406-421.

Konrad, J.M. and Law, K.T. 1987. Undrained shear strength from piezocone tests. Canadian Geotechnical Journal, 24 (3): 392-405.

Lin, L. and Adams. J. 2010. Strong motions from Nearby seismometer records of the Val-des-Bois, Québec, earthquake of June 23, 2010. Canadian Hazard Information Service Internal Report 2010-2.1, 23 pages plus digital Appendix.

Locat A, Leroueil S, Bernander S, Demers D, Jostad HP, Ouehb L (2011) Progressive failures in eastern Canadian and Scandinavian sensitive clays. Can. Geot. J. 48:1696-1712.

Ma, S. and Motazedian, D. 2012. Studies on the June 23, 2010 north Ottawa Mw 5.2 earthquake and vicinity seismicity. J. Seismol. 16:513-534.

Mitchell, R.J., Markell AR, 1974. Flowsliding in sensitive soils. Can. Geot. J. 11 (1):11-31

Odenstad, S. 1951. The landslide at Skottorp on the Lidan River February 2, 1946. Royal Swedish Geotechnical Institute Proceedings, No. 4, pp 7-39.

Perret, D., Mompin, R., Demers, D., Lefebvre, G. and Pugin, A.J.-M. 2013. Two large sensitive clay land-slides triggered by the 2010 Val-Des-Bois earthquake, Quebec (Canada) – Implications for risk man-agement. Poster, First Int'l Workshop on Landslides in Sensitive Clays (IWLSC), Quebec, Canada, 28-30 Oct. 2013.

Quinn PE, Diederichs MS, Rowe RK, Hutchinson DJ (2011) A new model for large landslides in sensitive clay using a fracture mechanics approach. Can. Geot. J. 48:1151-1162.

Rodríguez, C.E., Bommer, J.J., & Chandler, R.J., 1999. Earthquake-induced landslides: 1980–1997. Soil Dynamics and Earthquake Engineering 18: 325–346.

Roy S, Hawlayder B (2017) Finite element modelling of progressive and retrogressive failure of submarine slopes for varying angle of inclination. Proc. 70th Canadian Geotechnical Conference, Ottawa, Oct. 1-4, 2017

Tavenas, F. and Leroueil, S., 1987. State-of-the-art on laboratory and in-situ stress-strain-time behavior of soft clays. Proceedings of the International Symposium on Geotechnical Engineering of Soft Soils, Mexico City: 1-146.

Wang, B. 2016. Local shaking intensity of an earthquake that triggered Quyon Valley landslide 1020 cal yr BP. Proc. 69th Canadian Geotechnical Conference, Vancouver, 2-5 Oct. 2016. Paper #3684.

Wang, B. 2018. Failure mechanism of a prehistoric landslide in Champlain Sea clay at Breckenridge, Quebec. Proc. 71st Canadian Geotechnical Conference, Edmonton, 23-26 Sept. 2018. Paper #144.

Yu, H.S. and Mitchell, J.K., 1998. Analysis of cone resistance: review of methods. Journal of Geotechnical and Geoenvironmental Engineering, 124 (2): 140-149.

Zhang, X., Sloan SW, Onate E, 2018. Dynamic modelling of retrogressive landslides with emphasis on the role of clay sensitivity. Int. J. Numer. Anal. Methods Geomech. 2018:1-17. doi: 10.1002/nag.2815.